Label-free tungsten disulfide quantum dots as a fluorescent sensing platform for highly efficient detection of copper (II) ions*

Xuan Zhao(赵宣), Da-Wei He(何大伟)†, Yong-Sheng Wang(王永生)‡,
Yin Hu(胡音), Chen Fu(付晨), and Xue Li(李雪)

Key Laboratory of Luminescence and Optical Information, Beijing Jiaotong University, Beijing 100044, *China*

(Received 12 January 2017; revised manuscript received 23 February 2017; published online 20 April 2017)

A fluorescent probe for the sensitive and selective determination of copper ion (Cu^{2+}) is presented. It is based on the use of tungsten disulfide quantum dots (WS_2 QDs) which is independent of the pH of solution and emits strong blue fluorescence. Copper ions could cause aggregation of the WS_2 QDs and lead to fluorescence quenching of WS_2 QDs. The change of fluorescence intensity is proportional to the concentration of Cu^{2+}, and the limit of detection is 0.4 μM. The fluorescent probe is highly selective for Cu^{2+} over some potentially interfering ions. These results indicate that WS_2 QDs, as a fluorescent sensing platform, can meet the selective requirements for biomedical and environmental application.

Keywords: WS_2 quantum dots, photoluminescence, biosensor

PACS: 61.46.Df, 78.55.–m, 87.85.fk **DOI:** 10.1088/1674-1056/26/6/066102

1. Introduction

The detection of heavy metal ions in the areas of biological, chemical and environmental systems is very important, owing to their deleterious effects on human health.[1–3] The copper ion (Cu^{2+}), ranking behind zinc and iron, the third most abundant essential transition metal ion in the human body, plays a critical role in various biological processes.[4–6] The U.S. Environmental Protection Agency (EPA) and the World Health Organization (WHO) have set the limits of Cu^{2+} in drinking water to be 1.3 mg·L^{-1} (∼ 20 μmol·L^{-1}) and 2.0 mg·L^{-1} (∼ 30 μmol·L^{-1}), respectively.[7–9] The intracellular Cu^{2+} level in cellular homeostasis is directly related to the functions of proteins and various neurodegenerative diseases such as Menkes syndrome, Alzheimer's, Wilson's diseases, familial amyotrophic lateral sclerosis and Parkinson's.[10–13] Up to now, many research methods have been developed for the accurate determination of copper. The detection range is about 1.0 μM–4.0 μM.[14] In order to control the level of Cu^{2+} present in the environment and the ecosystem, there is a great demand for a reliable, simple and sensitive analytical method of detecting Cu^{2+} ions.

Since the discovery of graphene, great attention has been paid to two-dimensional (2D) materials comprised of layered transition metal dichalcogenides (TMDs) due to the high specific surface areas and outstanding electronic properties which are important for sensors, transistors, catalysis and energy storage applications.[15–30] Among the various types of 2D materials, tungsten disulfide (WS_2) has drawn a notable amount of interest in its ability to form monolayers. WS_2, with graphene-analogous crystal structure, is built up of W atoms sandwiched between two single layers of sulfur atoms though van der Waals forces and can be easily exfoliated along the layer plane.[31–33] Recent studies have reported that the bandgap of WS_2 can be transformed from an indirect gap (1.3 eV for bulk form) into a direct gap (∼ 2 eV for monolayer) when bulk WS_2 is thinned to the layer thickness.[34,35] This transition gives rise to the giant enhancement of the photoluminescence efficiency in WS_2 monolayer.

Currently, some efforts have been made to synthesize photoluminescent WS_2 materials and the methods can be divided into three ways including exfoliation of bulk crystals, substrate growth by chemical vapor deposition (CVD) and colloidal synthesis.[36–39] Compared with the latter two methods, the exfoliation of bulk materials not only has the advantages of time-saving, simplicity and no need for expensive instruments but also may introduce a larger perimeter–area ratio and more defects, which renders WS_2 excellent photoluminescence due to quantum confinement effect and edge effect.[40] WS_2 QDs would aggregate in the presence of Cu^{2+} because of electrostatic interactions, leading to the formation of WS_2 QDs-Cu^{2+} complex and fluorescence quenching. Herein, the probe will provide a sensitive and selective determination of copper ions in water samples.

*Project supported by the National Basic Research Program, China (Grant Nos. 2016YFA0202300 and 2016YFA0202302), the National Natural Science Foundation of China (Grant Nos. 61527817, 61335006, and 61378073), and the Beijing Municipal Science and Technology Committee, China (Grant No. Z151100003315006).

†Corresponding author. E-mail: dwhe@bjtu.edu.cn

‡Corresponding author. E-mail: yshwang@bjtu.edu.cn

© 2017 Chinese Physical Society and IOP Publishing Ltd

2. Experimental details

2.1. Instrumentation

Transmission electron microscopy (TEM) images were achieved by a JEM-1400 operating at 120 kV. The optical absorption spectrum of WS_2 QDs was obtained by a UV-3101 scanning spectrophotometer (Shimadzu, Japan) at room temperature. Fluorescence intensity was recorded on the luminescence spectrometer (Fluorolog-3). The x-ray photoelectron spectroscopy (XPS) measurement was carried out on PHI Quantera (PHI, Japan), the binding energy was calibrated with C1s=284.8 eV. Microplate reader (Thermo Scientific Multiskan MK3, Shanghai, China)

2.2. Synthesis of WS_2 QDs

WS_2 QDs were produced using a simple liquid exfoliation of bulk crystals. Briefly, 50 mg of WS_2 powder (Alfa Aesar) was added to 30 mL of distilled water in a 50-mL beaker and sonicated in an ultrasonic cell disruptor (400 W) for 4 h. Then, the precipitation with 30-mL NMP (1-methyl-2-pyrrolidinone) was sonicated in an ultrasonic bath continuously for 3 h. After that, the solution was centrifuged (9000 rpm, 30 min) and filtrated to remove large WS_2 sheets. Then the suspension was evaporated and re-dissolved in 50-mL water and stored at 4 °C.

2.3. MTT assay

The growth inhibition of the WS_2-treated HepG2 cells was measured using an MTT assay. The cells were seeded into 96-well cell culture clusters (Corning, NY, USA) at a density of 6×10^3 cells per well. After a 12-h incubation, the cells were treated with WS_2 for 6 h to 48 h. Thereafter, the cells were rinsed twice with PBS and incubated with 100 μL of a 0.5-mg/mL MTT solution at 37 °C for 4 h. After removing the supernatant, the formazan crystals formed by the MTT were dissolved with 150 μL of DMSO. The absorbance (A) at 490 nm was measured using a microplate reader. The cell viability was calculated from the following formula:

$$\text{Cell viability}(\%) = \frac{\text{A490, sample-A490, blank}}{\text{A490, control-a490, blank}} \times 100.$$

3. Results and discussion

3.1. Characterization of WS_2 QDs

The UV–vis absorption (blue line) and fluorescence emission spectra (red line) of WS_2 QDs are shown in Fig. 1(a). The ultra-violet–visible (UV–vis) absorption spectrum of WS_2 QDs in water shows a broad absorption band at approximately 275 nm. Moreover, when the excitation is 280 nm, the fluorescence emission spectrum has a strong peak at 457 nm. The inset image shows that the calculated band gap energy of WS_2 QDs is about 4.8 eV and blue fluorescence is observed when the

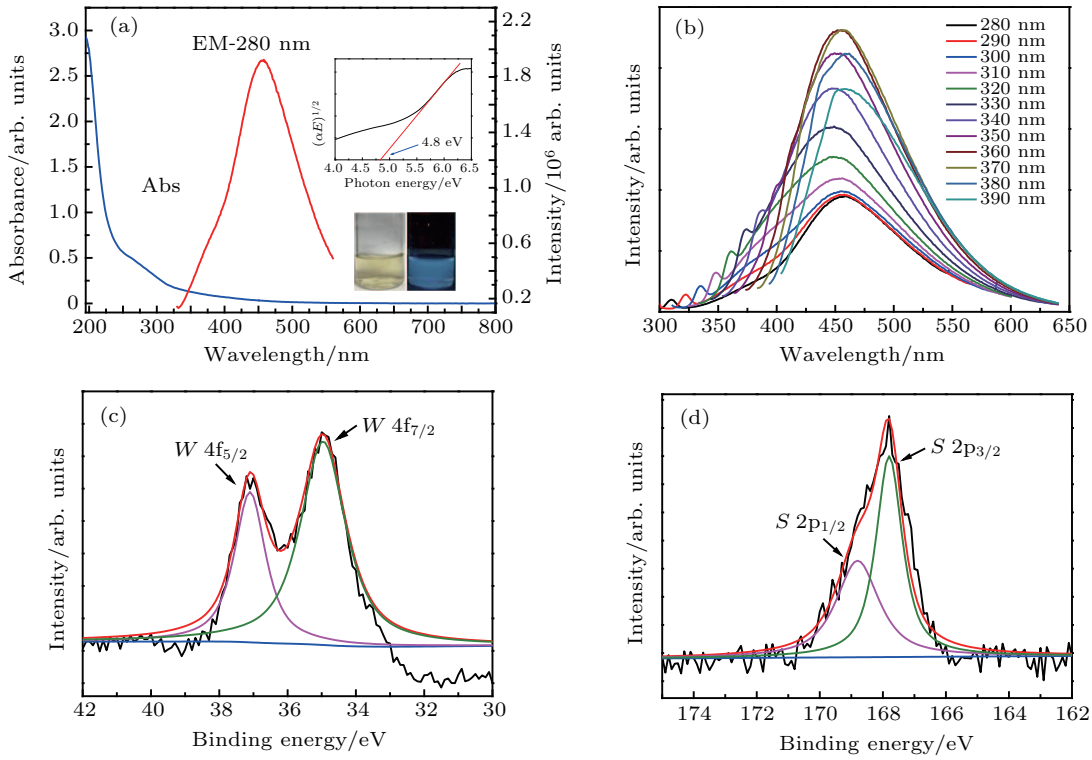


Fig. 1. (color online) (a) Absorption and PL emission spectra of WS_2 QDs (inset: calculated band gap energy of WS_2 QDs). (b) PL emission spectra of the WS_2 QDs obtained under excitations from 280 nm to 390 nm with 10-nm increase. The high resolution XPS survey spectra of the as-prepared WS_2 QDs. (c) *W* 4f and (d) *S* 2p spectra.

WS_2 QDs are irradiated with 365-nm UV light. Photoluminescence (PL) quantum yield of WS_2 QDs is 21.91%, using quinine sulphate as a reference at the excitation wavelength of 360 nm. The quantum yield of WS_2 QDs was calculated according to:

$$\frac{Y_x}{Y_s} = \frac{F_x}{F_s} \times \frac{A_s}{A_x},$$

where Y is the quantum yield, F is the measured integrated emission intensity, and A is the optical density. The subscript "s" refers to quinine sulphate, "x" denotes WS_2 QDs.

To further investigate optical properties, PL emission spectra of WS_2 QDs are recorded under various excitations. As shown in Fig. 1(b), with the excitation wavelength changing from 280 nm to 370 nm, emission peaks are blue-shifted from 459 nm to 447 nm, while the PL intensities are enhanced remarkably. A maximum fluorescence emission intensity can be obtained at 370 nm excitation. When the excitation wavelength ranges from 370 nm to 390 nm, the emission peaks shift from 447 nm to 462 nm with intensity decreasing gradually. This interesting result indicates that WS_2 QDs fluorescence may depend on the excitation wavelength.

To further explore the chemical property and composition of the WS_2 QDs, XPS characterization is carried out. As shown in Fig. 1(c), the W $4f_{7/2}$ and W $4f_{5/2}$ peaks for W^{4+} in WS_2 QDs can be observed at 37.1 eV and 35 eV, respectively. Meanwhile, the peaks at around 168.8 eV and 167.8 eV are attributed to the coexistence of S $2p_{3/2}$ and S $2p_{1/2}$ (Fig. 1(d)). Detailed compositional analysis results reveal that the atomic ratio (W:S) is 1:2.03.

3.2. Detection principle for copper ions

As shown in scheme 1 (see Fig. 2), Cu^{2+} can easily combine with WS_2 QDs through electrostatic interactions, which leads to the aggregation of QDs. The energy or electron will transfer from WS_2 QDs to Cu^{2+} and the fluorescence of QDs will be quenched. To confirm this principle, TEM and size distribution are performed. Figure 3(a) depicts the TEM images of WS_2 QDs.

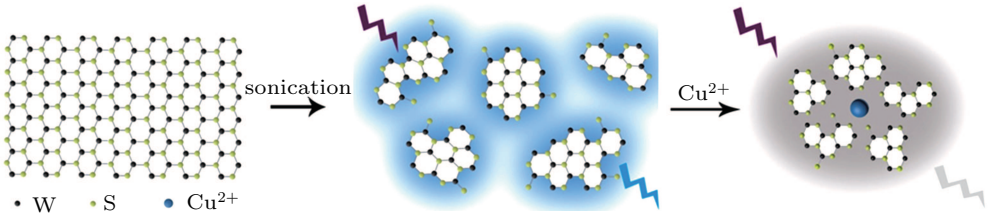


Fig. 2. (color online) Illustrations of the preparation scheme of WS_2 QDs and the detection of copper ions.

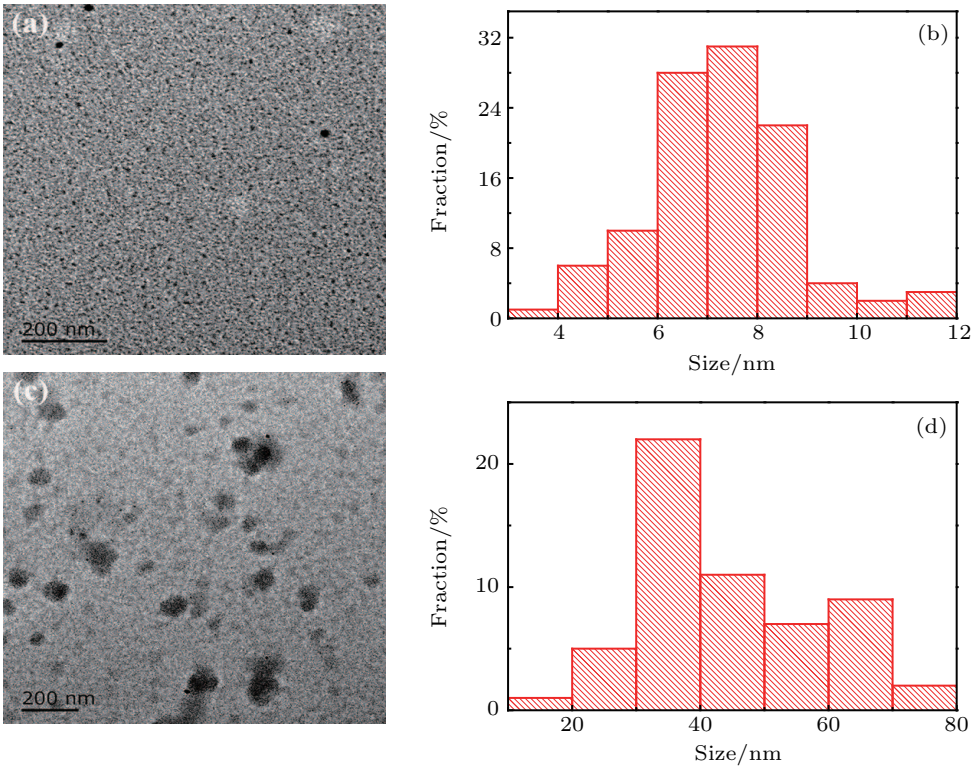


Fig. 3. (color online) (a) TEM image of WS_2 QDs. (b) Size distribution histogram of pure WS_2 QDs. (c) TEM image of WS_2 QDs with 200-μM Cu2+. (d) Size distribution histogram of WS_2 QDs with 200-μM Cu^{2+}.

Figure 3(b) shows that the diameters are mainly distributed in a range of 2 nm–12 nm (average 7 nm), suggesting that the as-prepared WS_2 QDs are uniformly arranged. When 200-μM Cu^{2+} are added (Fig. 3(c)), the WS_2 QDs aggregate obviously and the average diameter increases to about 40 nm (Fig. 3(d)). These results prove that Cu^{2+} can induce the aggregation of WS_2 QDs and quench the fluorescence.

3.3. Analytical performance of the sensor

To investigate sensitivity of the sensor, Cu^{2+} with concentrations ranging from 0 μM to 200 μM are analyzed by WS_2 QDs under 365-nm excitation wavelength. Figure 4(a) shows that the WS_2 QDs are sensitive to Cu^{2+} and the fluorescence intensity at 454-nm gradually decreases with the concentration of Cu^{2+} increasing. When the concentration of Cu^{2+} reaches 200 μM, the fluorescence intensity of WS_2 QD solution decreases to about 50% of its initial value. Figure 4(b) presents the relationship between the fluorescence intensity of WS_2 QDs and the concentration of Cu^{2+} (F_0 and F refer to fluorescence intensities at 365 nm in absence and presence of Cu^{2+}, respectively). The inset image indicates that a good linear relationship exists, which ranges from 0.2 μM to 1 μM with a high correlation coefficient ($R^2 = 0.986$). Based on $3\sigma/k$ (σ is the standard deviation of the corrected blank signals of the WS_2 QDs and k is the slope of the fitting line), the limit of detection of Cu^{2+} ions is estimated to be 0.4 μM, which is much lower than the maximum level (∼ 20 μM) set by the U.S. Environmental Protection Agency (EPA).

In order to study the practical applicability, the effect of pH on the fluorescence response of WS_2 QDs to Cu^{2+} is investigated. The experiments are carried out at a pH range from 2 to 12, with a concentration of WS_2 QDs fixed at 160 μg·ml^{-1} and 365-nm excitation wavelength (Fig. 4(c)), and Cu^{2+} at 100 μM (Fig. 4(d)). The results show that for both WS_2 QDs with and without Cu^{2+}, no obvious variation of the fluorescence emission is observed in the pH range 2 to 12, suggesting that the fluorescent sensor is independent of the pH of the solution.

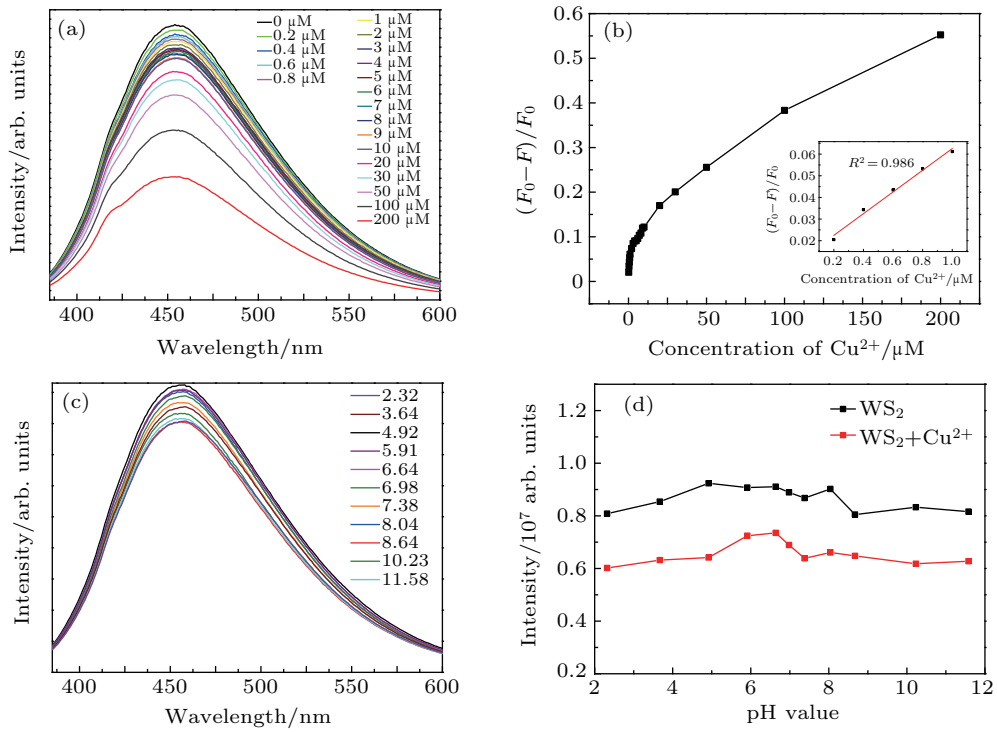


Fig. 4. (color online) (a) Emission spectra of WS_2 QDs in the presence of Cu^{2+} with concentrations ranging from 0 μM to 200 μM. (b) Plot of $(F_0 - F)/F_0$ of WS_2 QDs at 365 nm versus the concentrations of Cu^{2+} (inset: The calibration curve between concentration of Cu^{2+} and $(F_0 - F)/F_0$). (c) PL emission spectra of the WS_2 QDs at a pH range from 2 to 12. (d) Fluorescence intensity change of WS_2 QDs in the presence and absence of 100-μM Cu^{2+} at different pH values.

3.4. Selective detection of Cu^{2+} ions and cytotoxicity of WS_2

To assess the selectivity of Cu^{2+} detection, the PL response of the probe to potentially interfering substances (K^+, Na^+, Ca^{2+}, Ba^{2+}, Al^{3+}, Fe^{3+}, Ni^{2+}, Ag^+, Hg^{2+}, Zn^{2+}, SO_4^{2-}, Cl^-, NO^{3-}) is tested. The concentrations of the interfering substances and Cu^{2+} are tested at 200 μM under 365-nm excitation wavelength. As shown in Fig. 5(a), the interfering ions exhibit little influence on the fluorescence quenching rate of WS_2 QDs. This result demonstrates that sensing Cu^{2+} is hardly affected by these interfering ions and the fluorescent sensor is of very high selectivity for Cu^{2+} detection. Figure 5(b) shows the effect of WS_2 on the viability of HepG2 cells. The cells are cultured for 12 h and then incubated with

160 μg·ml^{-1} WS_2 for 6, 12, 24, and 48 h. Cell viability is determined by an MTT assay. The result indicates that WS_2 has no obvious cytotoxicity against HepG2 cell line *in vitro*.

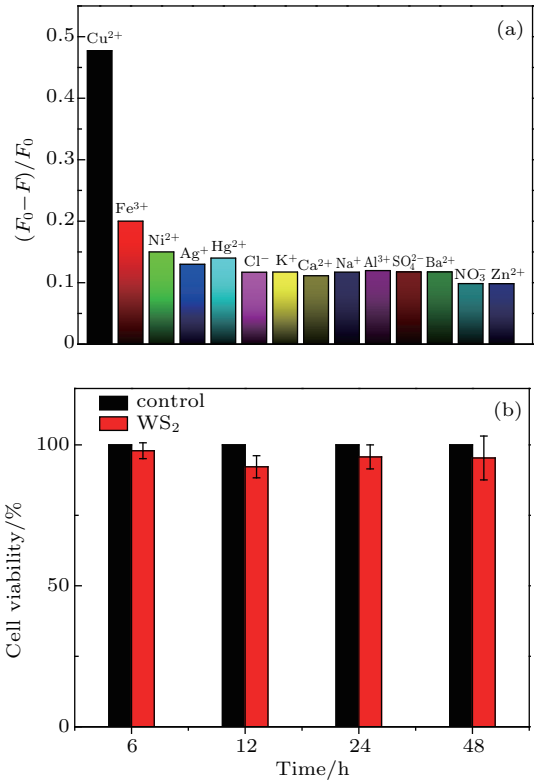


Fig. 5. (color online) (a) Various values of $(F_0-F)/F_0$ of WS_2 QDs solution in the absence and presence of 200-μM interfering substances (K^+, Na^+, Ca^{2+}, Ba^{2+}, Al^{3+}, Fe^{3+}, Ni^{2+}, Ag^+, Hg^{2+}, Zn^{2+}, SO_4^{2-}, Cl^-, NO^{3-}) under 365-nm excitation wavelength. (b) Effect of WS_2 on the viability of HepG2 cells. The cells are cultured for 12 h and then incubated with 160-μg·ml^{-1} WS_2 for 6, 12, 24, and 48 h. Cell viability was determined by an MTT assay.

4. Conclusions

In this paper, a simple but effective fluorescent probe, WS_2 QDs, is prepared for Cu^{2+} detection. The probe is independent of the pH of solution and hardly interfered with by other ions, upon excitation at 365 nm. The detection limit is estimated to be 0.4 μM, which is much lower than the maximum level (∼ 20 μM) set by the U.S. Environmental Protection Agency (EPA). These results indicate that WS_2 QDs could meet the requirements for biomedical and environmental application.

References

[1] Guo D, Dong Z, Luo C, Zan W, Yan S and Yao X 2014 *RSC Advances* **4** 5718
[2] Su Y, Shi B, Liao S, Qin Y, Zhang L, Huang M and Zhao S 2016 *Sensors and Actuators B: Chemical* **225** 334
[3] Guo Y, Wang Z, Qu W, Shao H and Jiang X 2011 *Biosens Bioelectron* **26** 4064
[4] Sun X, Liu P, Wu L and Liu B 2015 *Analyst* **140** 6742
[5] Liu Y, Zhao Y and Zhang Y 2014 *Sensors and Actuators B: Chemical* **196** 647
[6] Zong L, Song Y, Li Q and Li Z 2016 *Sensors and Actuators B: Chemical* **226** 239
[7] Wang F, Gu Z, Lei W, Wang W, Xia X and Hao Q 2014 *Sensors and Actuators B: Chemical* **190** 516
[8] Zhao J, Deng J, Yi Y, Li H, Zhang Y and Yao S 2014 *Talanta* **125** 372
[9] Li J J, Ji C H, Hou C J, Huo D Q, Zhang S Y, Luo X G, Yang M, Fa H B and Deng B 2016 *Sensors and Actuators B: Chemical* **223** 853
[10] Hu X X, Zheng X L, Fan X X, Su Y T, Zhan X Q and Zheng H 2016 *Sensors and Actuators B: Chemical* **227** 191
[11] Zhang C, Wan LY, Wu S, Wu D, Qin X and Ko F 2015 *Dyes and Pigments* **123** 380
[12] Bennur T, Khan Z, Kshirsagar R, Javdekar V and Zinjarde S 2016 *Sensors and Actuators B: Chemical* **233** 684
[13] Dong M, Liu C, Li S, Li R, Qiao Y, Zhang L, Wei W, Qi W and Wang H 2016 *Sensors and Actuators B: Chemical* **232** 234
[14] Liu Y, Deng M, Tang X, Zhu T, Zang Z, Zeng X and Han S 2016 *Sensors and Actuators B: Chemical* **233** 25
[15] Zhang X, Lei W, Ye X, Wang C, Lin B, Tang H and Li C 2015 *Mater. Lett.* **159** 399
[16] Xu S, Li D and Wu P 2015 *Adv. Funct. Mater.* **25** 1127
[17] Varoon K, Zhang X, Elyassi B, Brewer DD, Gettel M, Kumar S, Lee J A, Maheshwari S, Mittal A, Sung C Y, Cococcioni M, Francis L F, McCormick A V, Mkhoyan K A and Tsapatsis M 2011 *Science* **334** 72
[18] Schornbaum J, Winter B, Schießl S P, Gannott F, Katsukis G, Guldi D M, Spiecker E and Zaumseil J 2014 *Adv. Funct. Mater.* **24** 5798
[19] Pei L, Tao S, Haibo S and Song X 2015 *Solid State Commun.* **218** 25
[20] Lin H, Wang C, Wu J, Xu Z, Huang Y and Zhang C 2015 *New J. Chem.* **39** 8492
[21] Li Z, Ye R, Feng R, Kang Y, Zhu X, Tour J M and Fang Z 2015 *Adv. Mater.* **27** 5235
[22] Li B L, Chen L X, Zou H L, Lei J L, Luo H Q and Li N B 2014 *Nanoscale* **6** 9831
[23] Ke R, Zhang X, Wang L, Zhang C, Zhang S, Niu H, Mao C, Song J, Jin B and Tian Y 2015 *J. Solid State Electrochem.* **19** 1633
[24] Gopalakrishnan D, Damien D, Li B, Gullappalli H, Pillai V K, Ajayan P M and Shaijumon M M 2015 *Chem. Commun.* **51** 6293
[25] Gan Z X, Liu L Z, Wu H Y, Hao Y L, Shan Y, Wu X L and Chu P K 2015 *Appl. Phys. Lett.* **106** 233113
[26] Chen W, Zhao J, Zhang J, Gu L, Yang Z, Li X, Yu H, Zhu X, Yang R, Shi D, Lin X, Guo J, Bai X and Zhang G 2015 *J. Am. Chem. Soc.* **137** 15632
[27] Chen C, Qiao H, Lin S, Man Luk C, Liu Y, Xu Z, Song J, Xue Y, Li D, Yuan J, Yu W, Pan C, Ping Lau S and Bao Q 2015 *Sci. Rep.* **5** 11830
[28] Ali J, Siddiqui G U, Choi K H, Jang Y and Lee K 2016 *J. Lumin.* **169** 342
[29] Zhou H L, Yang W H, Wu Y P, Lin W, Kang J Y and Zhou C J 2015 *Chin. Phys. B* **24** 077301
[30] Dong Y F, He D W, Wang Y S, Xu H T and Gong Z 2016 *Acta Phys. Sin.* **65** 128101 (in Chinese)
[31] Zhao X, Ma X, Sun J, Li D and Yang X 2016 *ACS Nano* **10** 2159
[32] Dai Y, Yan X H, Wu X, Sha D W, Chen M, Zou H, Ren J and Cheng X N 2016 *Mater. Lett.* **173** 203
[33] Li Z, Jiang S, Xu S, Zhang C, Qiu H, Chen P, Gao S, Man B, Yang C and Liu M 2016 *J. Alloys Compd.* **666** 412
[34] Zhao X, Xia C, Wang T, Peng Y and Dai X 2015 *J. Alloys Compd.* **649** 357
[35] Tongay S, Fan W, Kang J, Park J, Koldemir U, Suh J, Narang DS, Liu K, Ji J, Li J, Sinclair R and Wu J 2014 *Nano Lett.* **14** 3185
[36] Thangaraja A, Shinde S M, Kalita G and Tanemura M 2015 *Mater. Lett.* 156 156
[37] Pumera M and Loo A H 2014 *TrAC Trends in Analytical Chemistry* **61** 49
[38] Zhou L, Yan S, Lin Z and Shi Y 2016 *Mater. Chem. Phys.* **171** 16
[39] Gao Y, Liu Z, Sun DM, Huang L, Ma LP, Yin LC, Ma T, Zhang Z, Ma X L, Peng L M, Cheng H M and Ren W 2015 *Nat. Commun.* **6** 8569
[40] Clark R M, Carey B J, Daeneke T, Atkin P, Bhaskaran M, Latham K, Cole I S and Kalantar-Zadeh K 2015 *Nanoscale* **7** 16763